Stress Corrosion Cracking in Welds of Al-Zn-Mg System 7NO1-T4 Alloy†

Toshio ENJO * and Toshio KURODA **

Abstract

An investigation has been made into the effect of microstructure on the stress corrosion cracking(SCC) in 3.5% NaCl + 0.5% H_2O_2 aqueous solution for Al-Zn-Mg system 7N01-T4 alloy welds. Its susceptibility to SCC is known to be affected by microstructure. The microstructure consisting of G.P. zones has high susceptibility to SCC, and that consisting of η'precipitates and η phase has low susceptibility to SCC. The microstructure in which G.P. zone and a few η'precipitates or η'phase are mixed, has lower susceptibility to SCC than that consisting of G.P. zones only. SCC of the welds occured at the area of G.P. zone microstructure such as the weld bond area and base metal of non-heat affected zone, but the SCC hardly occured at the area where only a few η'precipitates or η phase existed in the weld heat affected zone. The fracture morphology of SCC in the microstructure consisting of G.P. zones showed intergranular fracture with plain surface, while that of SCC in the microstructure consisting of η'precipitates or η phase seemed to show intergranular fracture assosiated with grain boundary precipitates.

KEY WORDS: (Al Zn Mg Alloy) (Heat Affected Zone) (Stress Corrosion Cracking) (Fractography) (Metallography)

1. Introduction

Al-Zn-Mg system 7NO1-T4 alloy has high tensile strength above 32 kg/mm^2 and has been widely used to various structural materials for the reason of light weight characteristics. This alloy has high susceptibility to stress corrosion cracking (SCC) in the environment such as sea water, and the SCC is well known to associate with microstructure such as grain boundary precipitates[1)2)], precipitate free zone (PFZ)[3)4)], precipitates in grain[5)6)] and relatively insoluble compounds[7)] up to the present day. But the relation between the SCC and their factors has been hardly clear with regard to the welds. That is, the weld heat affected zone (HAZ) and weld metal will be suffered the complicated thermal history, and the complication of microstructure has prevented the proceeding of the investigation of SCC in welds. Therefore, actual SCC of welds can be hardly explained on the basis of individual effect of factors above mentioned. Then in this investigation, the microstructure change by various heat treatment concerning the HAZ was evaluated with the concentration change of Zn and Mg from the matrix by means of electrical resistivity. And the relation between the change in microstructure and SCC and, the fracture morphology was investigated, on the basis of the results, the SCC of welds was discussed.

2. Experimental Procedure

The material used in this investigation is commercially Al-Zn-Mg system 7NO1-T4 alloy and the chemical compositions are shown in **Table 1**. 7NO1(A) was used for

Table 1 Chemical compositions of materials used (wt%)

Materials	Cu	Si	Fe	Mn	Mg	Zn	Cr	Ti	Zr	Al	*	**
7N01 (A)	Tr	0.08	0.14	0.37	1.3	5.1	0.22	0.02	0.15	Bal.	34†	T4
7N01 (B)	Tr	0.07	0.15	0.47	1.21	4.96	0.22	0.05	0.06	Bal.	16†	T4

* Plate thickness
** Heat treatment

SCC test of short transverse direction (ST) specimen, and 7NO1(B) was used for the SCC test of long transverse(LT) direction specimen and the welds. The specimen dimensions for the SCC of base metal are shown in **Fig. 1(a)**, that of welds is shown in **Fig. 1(b)**. In this investigation, to make clear the propagation process of SCC is important, and then the specimen dimensions was with notch in order to prevent the incubation time up to crack initiation of SCC. In the case of welds, the change in microstructure occurs continuously in the HAZ. And then, the plain specimens with welds were used in order to investigate which microstructure region occur SCC. The SCC test was

† Received on September 27, 1980
* Professor
** Research Instructor

Transactions of JWRI is published by Welding Research Institute of Osaka University, Suita, Osaka, Japan

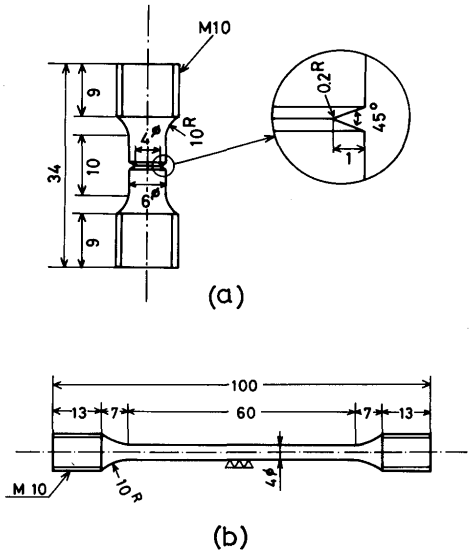

Fig. 1 Specimen dimensions for SCC test.
(a) Base metal (b) Welds

carried out in 3.5%NaCl + 0.5%H_2O_2 aqueous solution under the dead load, and the fracture time was measured. PH at the first time of the test was about 4.5. The fracture surface obtained by the SCC test was observed in detail by means of scanning electron microscope.

For the heat treatment of base metal, the salt bath was used.[8] The precipitation behavior of precipitates such as η' transition phase or η equilibrium phase and the relatively insoluble compounds were investigated by means of transmission electron microscope using thin foil and electrical resistivity measurement of conventional potentiometric method. Thin foils for transmission electron microscopy were prepared using a jet polishing technique. In welding, DCSP TIG method (heat input 30000 J/cm) and electron beam (EB) welding method (heat input 1000 J/cm) was carried out, and the plain specimens with welds cut out from the weldments as shown in **Fig. 1-b**.

3. Results and Discussion

3.1 Effect of solution or aging temperature on the stress corrosion cracking

Generally, the hardness doesn't restore by natural aging after welding, so called, softening zone occurs at the region heated at 200~300°C in the HAZ of Al-Zn-Mg alloy.[9][10] But, the SCC of HAZ involving the softening zone has been hardly investigated in detail. Firstly, concerning the microstructure of HAZ, the SCC test was carried out about the each microstructure of non-heat affected zone, the softening zone and the region solution-ized adjacent to the weld bond. **Figure 2** shows the transmission electron micrographs using thin foil, which 7NO1-T4 material was solution-treated 2 hrs at 560°C, water quenched at 0°C, and aged at 210°C for 2 hrs.
Giant particles show the relatively insoluble compounds[7] formed by the impurities such as Fe, Si and additional elements such as Cr, Mn, Zr. The η phase precipitates at the grain boundary. As shown in **Fig. 2(b)**, η' transition phase of the size about 20 Å precipitates in the grain. Now, the relatively insoluble compounds was present only, according to the transmission electron micrograph, and G.P. zones generate according to the electrical resistivity for as received material (T4). At the aging treatment of 250°C, η phase precipitated in the grain and at the

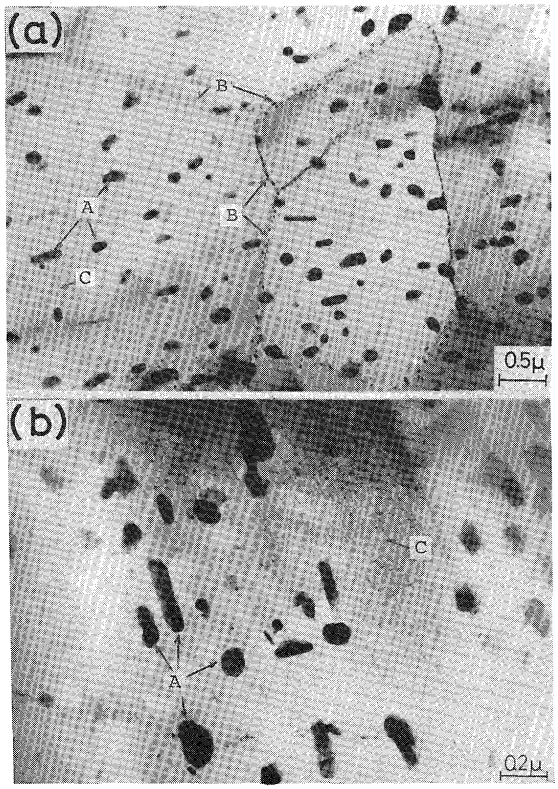

Fig. 2 Transmission electron micrographs of the specimen aged at 210°C for 2 hrs after solution heat treatment at 560°C for 2 hrs. (A: Relatively insoluble compounds, B: η phase, C: η' precipitates)

grain boundary. The identification of their precipitates was carried out on the basis of the morphology[12][13], and η phase was reconfirmed by X-ray diffraction analysis and electron beam diffraction technique, too. And then, T4 specimens, the specimens water quenched and aged at room temperature for 30 days after solution treatment 2 hrs at 560°C or 380°C, and the specimens aged at 210°C

or 250°C for 2 hrs (This time is that the decrease of the resistivity hardly occurs) were prepared respectively. And it was investigated on the effect of solution or aging temperature on the SCC for ST direction specimens of 7NO1-T4 alloy. The results are shown in **Fig. 3**.

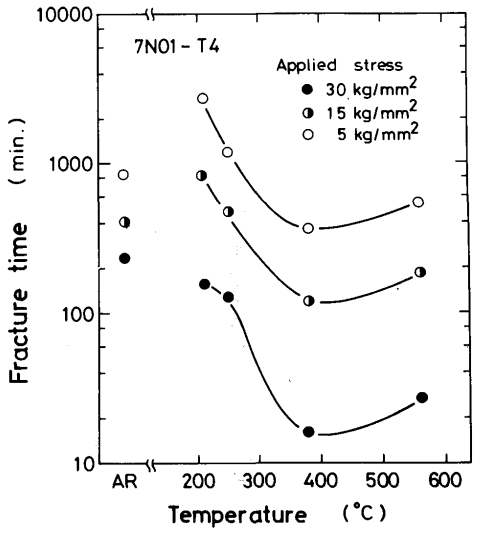

Fig. 3 Effect of aging or solution temperature on the fracture time of SCC for ST direction specimens of 7N01-T4 alloy.

Well, 0.2% proof stress of the each specimen heat-treated were summerized as follows. T4 material was 33 kg/mm^2, the solution-treated specimen at 380°C for 2 hrs was 24 kg/mm^2, the solution-treated specimen at 560°C for 2 hrs was 21 kg/mm^2, the specimen aged at 210°C for 2 hrs was 18 kg/mm^2, and the specimen aged at 250°C for 2 hrs was 18 kg/mm^2. The applied stress as same that the notch root region was yielded was evaluated on the basis of the 0.2% proof stress of each specimen by means of finite element method. The SCC test under the applied stress was carried out. As the results, for each specimen, the fracture time was about the same time as the results of 5kg/mm^2 shown in **Fig. 3**. In the actual welds, the region with their microstructure can be hardly stress-applied under each their yield stress, and can be stress-applied under the constant load or weld residual stress. Then, the effect of heat treatment on the SCC under three kinds of applied stress was investigated firstly. The fracture time of the SCC for solution-treated specimens was shorter than that of the specimens aged at 210°C or 250°C under every applied stress. The facture time of the SCC for the specimens aged at 210°C is longer than that of the specimens aged at 250°C. And the fracture time of SCC for solution-treated specimens is shorter than that of as-received material (T4). It is known that the G.P. zones radius during room temperature aging becomes larger as the aging time becomes longer.[14] The base metal (T4) used in the present investigation has been aged more than six months. The radius of G.P. zones for T4 material is considered to be larger than that of the solution-treated specimen. Therefore, the fracture time of SCC is considered to have become longer than that of the solution-treated specimens. The specimen solution-treated at 380°C keeps flat grain boundaries by rolling process, but, the specimen solution-treated at 560°C has been partially recrystallized. Therefore, in the SCC of the solution-treated specimen at 560°C, the crack propagation is inpeded by the recrystallization structure as shown in **Fig. 7(a)**. Consequently, it is considered that the fracture time of the specimen solution-treated at 560°C was longer than that of the specimen solution-treated at 380°C.

3.2 Stress corrosion cracking in the mixture structure of the precipitates and G.P. zones

Considering the welds and HAZ of 7NO1-T4 alloy in conventional welding procedure, the weld heat input is from 10000 J/cm to 30000 J/cm, the holding time at 210°C or 250°C is only 2~3 minutes,[15] and then the HAZ has the mixture structure of G.P. zones, η' precipitates and η phase.[9)15] The region heated at 210°C or 250°C is considered to form the softening zone. In the case of the welds, the microstructure in the softening zone can be changed continuously by the complicated factor such as heat input, plate thickness, cooling time so on. But, the mixture state of G.P. zones and the precipitates

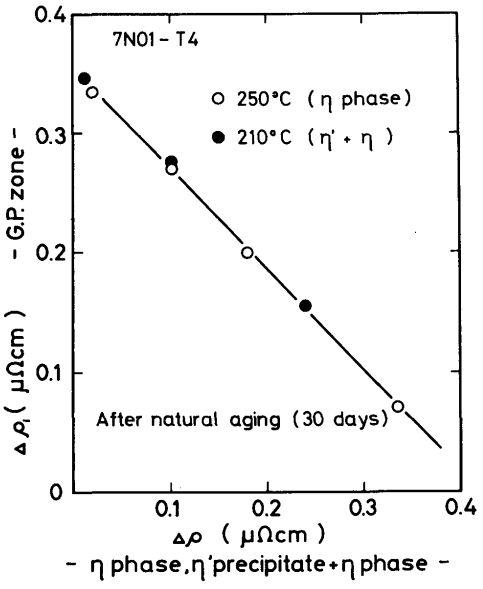

Fig. 4 Effects of η' precipitates and η phase on the generation of G. P. zones.

in the HAZ has been hardly evaluated. And then in the present investigation, considering the softening zone, the precipitation amount of η' or η phase at 210°C or 250°C were evaluated by the value of the electrical resistivity, and the mixture amount of their precipitates and G. P. zones were evaluated on the basis of the relation between the precipitates amount ($\Delta\rho$) and G.P. zones amount ($\Delta\rho_1$) after natural aging for 30 days. The results are shown in **Fig. 4**. The horizontal axis shows the resistivity change ($\Delta\rho$) due to that the precipitation occurs, when the specimens were aged at 250°C for 1 min., 5 min, 10 min, and 30 min, respectively, and the change ($\Delta\rho$) due to that the precipitation occurs, when the specimens were aged at 210°C for 1 min, 10 min, and 30 min. respectively. The longitudinal axis shows the amount of G. P. zones ($\Delta\rho_1$) after natural aging of 30 days on the each precipitates amount. The rate of precipitation at 210°C aging was slower than that at 250°C aging. But, in spite of the morphology change of the precipitates, if the precipitation is the same amount in the electrical resistivity change, the amount of G. P. zones after natural aging 30 days shows the same value. As the precipitates such as η' or η phase precipitates more, the amount of G. P. zones ($\Delta\rho_1$)

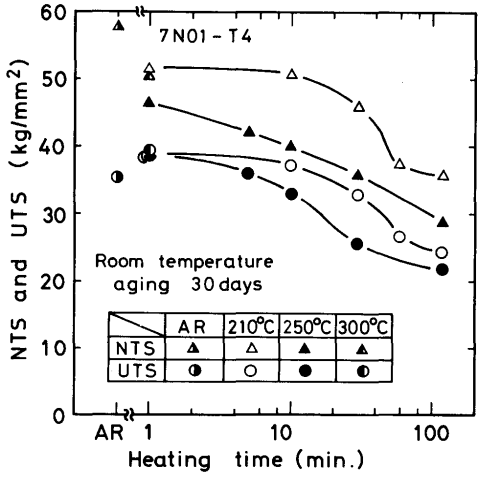

Fig. 5 Effect of heating time at various temperatures on the NTS and UTS.

decrease inversely. According to Kawano[14], the radius of G. P. zones in every heat-treated specimen was the same value, when the specimens water-quenched or air cooled from the solution temperature or 250°C were aged at room temperature respectively. Consequently, the G. P. zones radius is considered to have the same value on the specimens precipitated η' precipitates and η phase in the present investigation too. The mechanism of strengthening of T4 material used is due to the G. P. zones generated at room temperature. And as the precipitates such as η' or η

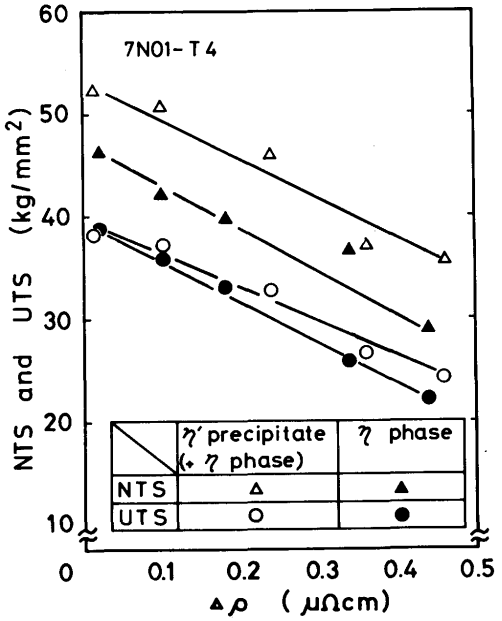

Fig. 6 Effects of η' precipitates and η phase on the NTS and UTS.

phase increase, the generation of the G. P. zones decreases, and the strength and hardness after natural aging decreases. This is considered to be softening zone in the HAZ.

Figure 5 shows the effect of heating time at various temperatures on the NTS and UTS after natural aging of 30 days. In the case of 210°C aging, NTS and UTS hardly change till 10 min. aging. In the case of 250°C aging, NTS and UTS decrease with increasing the aging time. Consequently, the softening zone in the HAZ is due to about 250°C heating. **Figure 6** shows the effect of electrical resistivity change upon the precipitation on the NTS and UTS after natural aging 30 days. The precipitates at 250°C is η phase, and that at 210°C is mainly η precipitates. As the η orecipitates or η phase increase in the matrix, the generation of G. P. zones decreases, and NTS and UTS decrease, by means of electrical resistivity measurement.

Figure 7 shows the effects of η' precipitates and η phase on the fracture time of SCC for LT direction specimens. The amount of precipitates such as η' precipitates and η phase were evaluated by means of electrical resistivity measurement. Well, as the amount of precipitates increases, the generation of G.P. zones decreases as shown in **Fig. 4**. In the case of applied stress at 30 kg/mm^2, as shown in **Fig. 7(a)**, the fracture time of SCC can be increased by the increase in precipitate amount, up to 50% of whole precipitation amount at 210°C and 40% of whole precipitation at 250°C. In more than the amount of the precipitates, the generation of G. P. zones is slightly

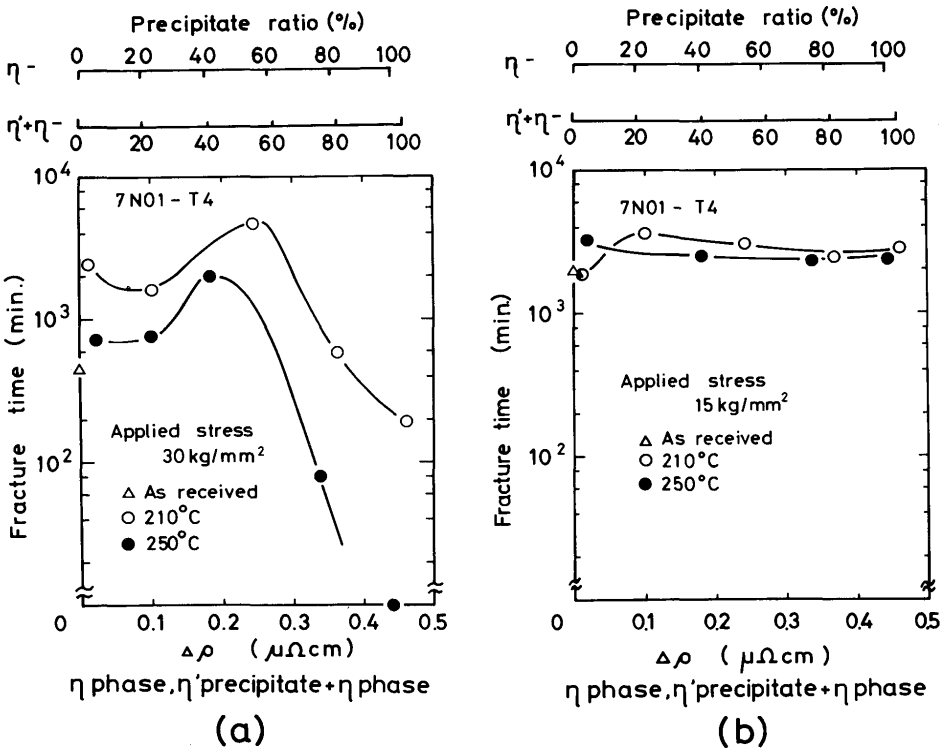

Fig. 7 Effects of η' precipitates and η phase on the fracture time of SCC for LT direction specimens

decreased by the precipitation of η' or η phase, and the strength decreases, the plastic deformation occurs widely, and then the fracture time of SCC was considered to have decreased. The other way, in the case of the applied stress at 15kg/mm^2, the facture time of SCC for the mixture structure of G. P. zones and the precipitates is longer than that of G. P. zones only. But according to the electrical resistivity, even though the amount of η' or η phase increase, the fracture time of SCC by the precipitation hardly increase. The fracture time of SCC for the specimen aged at 210°C is longer than that for the specimen aged at 250°C. According to Murakami et al[2], the grain boundary precipitates ($MgZn_2$) works actively in electrochemistry in 3.5%NaCl + 0.5%H_2O_2 aqueous solution, the crack propagates along the interface of the grain boundary precipitates and the matrix, and at the precipitates themselves. In the present investigation, the precipitation state has been evaluated by the concentration change of Zn and Mg in electrical resistivity. As shown in **Fig. 7**, even though the amount of precipitation is the same each other, the fracture time of SCC can be changed by the applied stress. This is considered to be due to the complication of the factor such as grain boundary precipitates, the width of PFZ and the G. P. zones in the grain. Consequently, the SCC will hardly occur at the softening zone heated at 210°C or 250°C in the HAZ.

3.3 Stress corrosion cracking in welds

Generally, the welds is composed of weld metal (A), the region heated above the solution temperature (B), the region heated at the temperature between the solution temperature and solvus temperature of G. P. zones (C) and the region heated below the solvus temperature of G. P. zones such as non heat affected zone (D)[15]. As the weld heat input increases, the decrease of hardness in the softening zone becomes conspicuous more in the area (C). **Figure 8** shows the stress corrosion cracking curves for the plain specimens with TIG welds and EB welds. In the case of EB welds, the weld heat input was about 1000 J/cm, therefore, the microstructure change is considered to be hardly present, because of the thermal cycle owing to rapid heating and cooling in the HAZ. Consequently, the welds has the same microstructure as that of as-received material (T4). The other way, in the case of TIG welds, the weld heat input was 30000 J/cm, and because of considerably larger heat input, the each area of (A)~(D)

was recognized distinctly.[15] Consequently, the SCC under the higher applied stress occured at the base metal for EB welds and occured at the bond region with partially recrystallized structure for TIG welds. The fracture time of SCC for TIG welds was longer than that for EB welds. The other way, on approaching to the lower applied stress, the fracture time of SCC showed the same value as in TIG welds, EB welds and as-recieved specimen (T4) respectively, the fracture position was the region of microstructure composed of G. P. zones. And the SCC hardly occued in the area containing of η'precipitates and η phase in the region (C). The results agree with the results expected from **Fig.3** and **Fig. 7**.

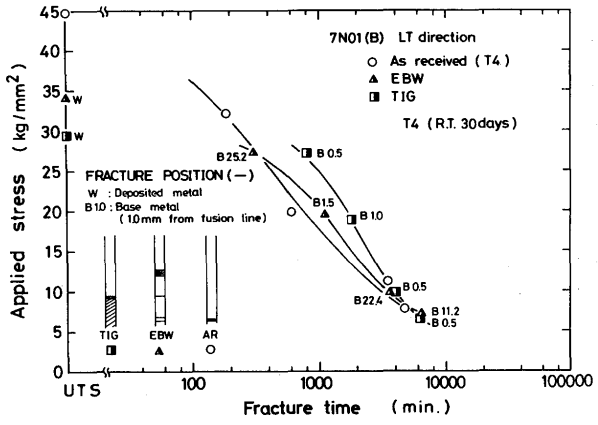

Fig. 8 Stress corrosion cracking curves for TIG welds and EB welds.

3.4 Fractography of the stress corrosion cracking

Generally, the SCC of aluminum alloy is well known to show the intergranular fracture[2)17)]. Then, in this section, the fracture path of SCC was investigated. The results are shown in **Fig. 9**.

Figure 9(a) shows the microstructure showing crack profile of SCC for ST direction specimens solution-treated at 560°C for 2 hrs, and aged at room temperature for 30 days. The recrystallized structure partially occured and the microstructure was G. P. zones. The crack was stopped by the recrystallization grain, and propagated into the grain partially. But main crack propagated along the grain boundary. For LT direction specimen as shown in **Fig.9(b)**, the crack was stopped by the flat grain of non-recrystallization, and the crack propagated along the other grain boundary after branching. Their fracture morphologies in the SCC are shown in **Fig. 10**.

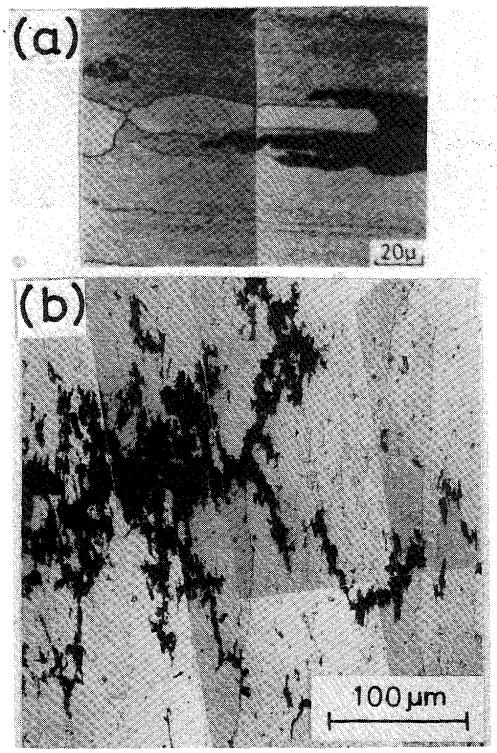

Fig. 9 Microstructure showing crack profile of SCC.
(a) ST direction specimen, (b) LT direction specimen

Figure 10 (a) shows the fracture morphology of SCC in ST direction specimens, and **Figure 10 (b)** shows the fracture morphology of LT direction specimen. In any of them, the region of mark (A) shows the SCC, and the region of mark (B) shows the fast fractured region. Their morphologies can be distinguished clearly by fractography. In the fast fractured region, the morphology shows the dimple pattern, the relatively insoluble compounds and inclusions existed at the dimple bottom. In the region of SCC in LT

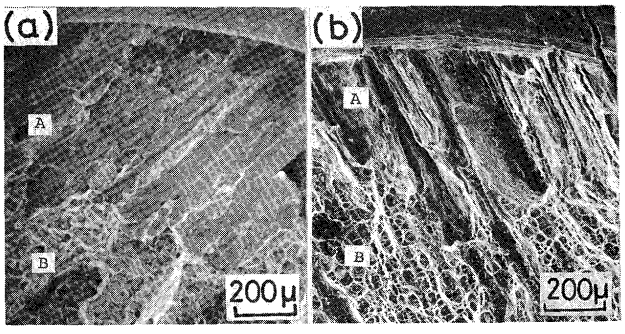

Fig. 10 Fractographs of stress corrosion cracking
(a) ST direction specimen (b) LT direction specimen

direction specimen, many subcracks along the slender, flat grain boundary are recognized. This can be understood from the fracture path of **Fig. 9**. Now, it is not clear whether the path of main crack is along the intergranular or at the transgranular. The other way, for ST direction specimen, the region of SCC is considerably flat, the fracture morphology shows both the intergranular and transgranular fracture.

In the present investigation, the difference of the fracture morphology between the specimen composed of G. P. zones only and the specimens composed of the precipitates such as η' or η phase were evaluated by fractography. **Figure 11** shows the fractographs of SCC in ST direction specimens, which solution-treated at 380°C and 560°C, and aged at room temperature for 30 days. In both specimens, the microstructure is composed of G. P. zones only. The fracture morphology shows considerably flat intergranular fracture, and the surface hardly had been corroded though the corrosion particles merely adhered. **Figure 12** shows the fractographs of SCC in ST direction specimen aged at 210°C or 250°C for 2 hrs.

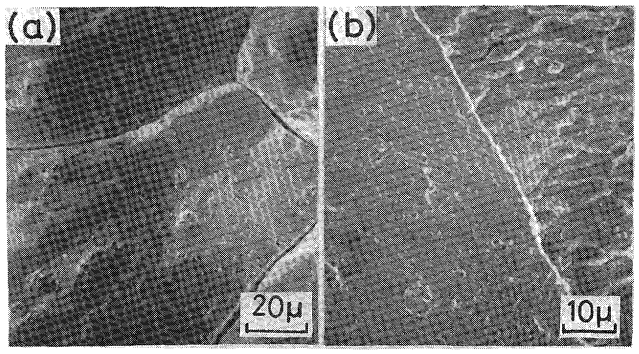

Fig. 11 Fractographs of SCC in ST direction specimens.
(a) Solutionized at 560°C (b) Solutionized at 380°C

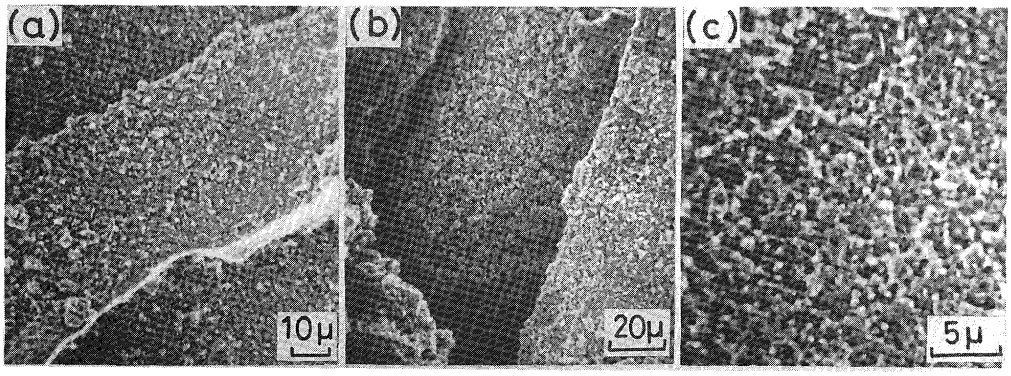

Fig. 12 Fractographs of SCC in ST direction specimens.
(a) Aged at 210°C for 2 hrs. (b) Aged at 250°C for 2hrs.
(c) Enlarged (b).

The η phase precipitated at the grain boundary in both specimen of aging according to the transmission electron micrographs. The facture surfaces were corroded considerably as shown in the **Fig. 12 (c)**, many micropores on the fracture surface can be observed. Such a result has already observed by Murakami et al[2], further the fracture morphology is considered to show that the corrosions occured at the interface of the grain boundary between precipitates and the matrix, or at the precipitates themselves, or at the surrounding area of the precipitates considering from the results of Jacobs[17]. Consequently, in the case that the grain boundary precipitates are present, the fracture morphology of SCC shows the intergranular fracture with corrosion associated with the grain boundary precipitates, but that composed of G. P. zones shows intergranular fracture without corrosion. The SCC of the welds occured at the G. P. zones structure such as weld bond or non heat affected zone solution-treated respectively. The fracture morphology of SCC showed the intergranular fracture without corrosion.

4. Conclusion

An investigation has been made into the stress corrosion cracking of Al-Zn-Mg system 7NO1-T4 alloy welds in 3.5%NaCl + 0.5%H_2O_2 aqueous solution. The results obtained in this investigation are summerized as follows.

(1) By means of electrical resistivity, the generations of G. P. zones after natural aging decrease, as the precipitation at 210°C or 250°C increases. This is considered to be the cause of the softening zone in the heat

affected zone.

(2) In the mixture structure of G. P. zones and the precipitates such as η' or η phase, the fracture time of stress corrosion cracking depends on the amount of the precipitates strongly under the higher applied stress. But, under the lower applied stress, the fracture time hardly depend on the precipitates. The fracture time of stress corrosion cracking in the mixture structure is longer than that of G. P. zones only.

(3) In EB welds and TIG welds, the fracture position of the stress corrosion cracking is the region of the microstructure composed of G. P. zones such as the weld bond or non-heat affected zone. The weld metal was hardly corroded and hardly occured stress corrosion cracking.

(4) The fracture morphology of the stress corrosion cracking showed flat intergranular fracture in the microstructure composed of G. P. zones, and intergranular fracture associated with grain boundary precipitates in the microstructure composed of the precipitates such as η' or η phase. The fracture morphology of the weld showed the intergranular fracture without corrosion, and then the results proved that the stress corrosion cracking occured at the microstructure composed of G. P. zones only.

Acknowledgement

The authors wish to thank Mr. M. Mishima and Mr. K. Ishimoto for their variable contribution in this work. The support of the Light Metal Educational Foundation is grately acknowledgement.

References

1) Poulose, P.K., J.E. Morral and A.J. Mchevily ; Met. Trans., 5, 1393 (1974).
2) Miyamoto M. and Y. Murakami; J. Japan Inst. Metals, 37, 394 (1969) (In Japanese)
3) Kent K.G.; J. Inst. Metals, 97, 127 (1969)
4) Sedriks A.J., P.W.Slattery and E.N.Pough; Trans. ASM, 62 238 (1969)
5) Tanaka K. T. Saito; J.Japan Inst. of Light Metals, 19, 55 (1969) (In Japanese)
6) Markus O. Speidel; Met. Trans. 6A, 631 (1975)
7) Miyamoto Y.M.Hirano; J. Japan Inst. of Light Metals, 26, 501 (1976) (In Japanese)
8) Enjo T.T.Kuroda and H.Shinonaga; Trans. JWRI 7, 173 (1978)
9) Mizuno M. M. Kikuchi, Y. Baba and T. Fukui; J. Japan Inst. of Light Metals, 26, 564 (1976) (In japanese)
10) Tanaka K. and T. Satoh ; J. Japan Inst. of Light Metals, 19, 336 (1969) (In Japanese)
11) Fukui T. H. Yoshida and Y. Baba; J. Japan Inst. of Light Metals, 28, 57 (1978) (In Japanese)
12) Embury J. D. and R.B. Nicholson; Acta Met. 13, 403 (1965)
13) Thomas G. and J.Nutting; J. Inst. Metals, 88, 81 (1959-1960)
14) Kawano O.; J. Japan Inst. of Light Metals, 20, 148 (1970)
15) Enjo T. T. Kuroda and K. Ishimoto. To be published
16) Hagiwara T. T. Fukui, T. Sugiyama and S. Terai ; J. Japan Inst. of Light Metals, 19, 47 (1969) (In Japanese)
17) Jacobs A. J.; Trans. ASM, 58, 579 (1965)